

# AN3009: Characterization of self-associating antibody solutions at high concentrations with CG-MALS

Sophia Kenrick, Ph.D. and Daniel Some, Ph.D., Waters | Wyatt Technology

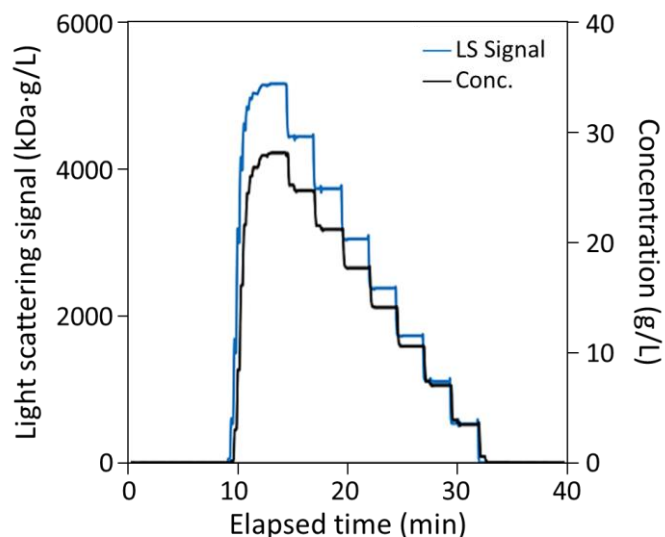
## Summary

The characterization of therapeutic protein formulations is essential for the development of novel biopharmaceuticals. In particular, solution viscosity and colloidal stability may be adversely impacted by attractive self-interactions among protein molecules. In this study, we quantified the self-association affinity and stoichiometry of three antibody formulations (mAbs A, B, and C) in their corresponding formulation buffers using **composition-gradient multi-angle light scattering (CG-MALS)**.

Experiments were performed with a **Calypso® concentration-gradient system**, a **DAWN® multi-angle light scattering (MALS) detector**, and **Optilab® dRI detector** with high concentration range (HC model). The Calypso automated the generation of 8-9 concentrations of each antibody up to concentrations ~40 mg/mL and delivered them to downstream detectors. Additional measurements of higher concentrations were made with a **microCuvette®**. The light scattering and concentration data were collected with the **CALYPSO™ software** and fit to an appropriate interaction model, taking into account both specific attractive interactions and nonspecific repulsive interactions, expressed as a positive second virial coefficient,  $A_2$ .

The viscosity of the antibody stock solutions correlated well to the measured attractive interactions among the molecules. The lowest viscosity formulation (mAb A) exhibited only repulsive interactions, quantified by a second virial coefficient of  $7.3 \times 10^{-5} \text{ mol} \cdot \text{mL} / \text{g}^2$  which is slightly more repulsive than the pure excluded-volume  $A_2$  of  $\sim 5.0 \times 10^{-5} \text{ mol} \cdot \text{mL} / \text{g}^2$ . In contrast, mAbs B and C exhibited significant self-association; the best fit to the light scattering data indicated that the antibodies form weak dimers, which associate further to form higher order

oligomers. This self-association is believed to be the mechanism behind increased viscosity at the formulation concentration.



Typical light scattering and measured concentration for CG-MALS gradient automated by the Calypso.

	$A_2$ ( $\text{mol} \cdot \text{mL} / \text{g}^2$ )	Dimerization $K_D$ ( $\mu\text{M}$ )	ISA $K_D$ ( $\mu\text{M}$ )
mAb A	$7.13 \times 10^{-5}$	--	--
mAb B	$4.47 \times 10^{-5}$	280	180
mAb C	$5.09 \times 10^{-5}$	400	130

Best fit parameters for self-interactions of mAbs A, B, and C. Samples B & C exhibit transient association forming fairly large oligomers.

## Introduction

Recent research suggests that weak protein-protein interactions play a key role in the viscosity and colloidal stability of a protein formulation<sup>1</sup>. Batch (unfractionated) multi-angle light scattering (MALS) is uniquely suited to quantifying these interactions, enabling measurements in solution at the concentration of interest without tagging, immobilization, or other sample modifications<sup>2,3</sup>. In this study, we applied automated composition-gradient multi-angle light scattering (CG-MALS)<sup>4</sup> to the characterization of the intermolecular interactions of three antibody formulations to evaluate the correlation of these interactions with the formulation viscosity.

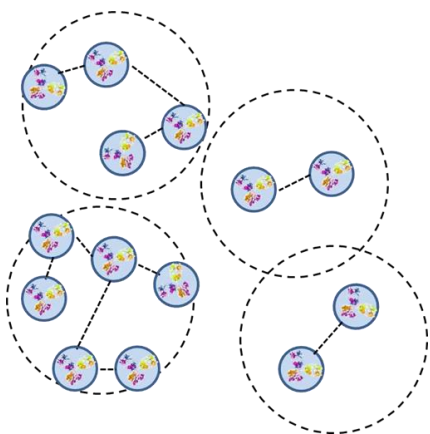
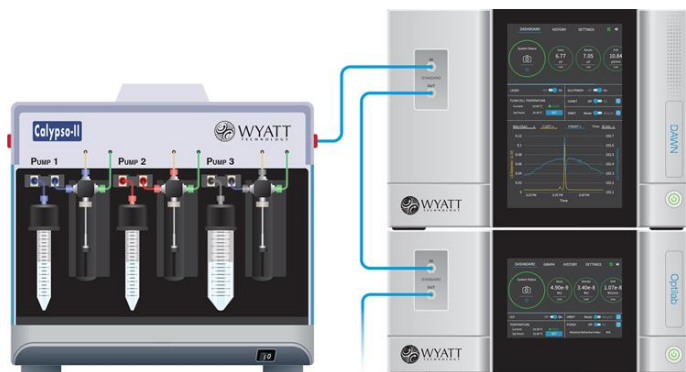


Figure 1: Antibody molecules associate with nearest neighbors into loose networks described as quasi-specific oligomers.

## Materials and Methods

Antibody and buffer solutions were kindly provided by MedImmune, LLC (Gaithersburg, MD). Light scattering data for each antibody was measured in its respective formulation buffer at 15-20 concentrations. For mAb A, all dilutions were automated by the Calypso. For mAbs B and C, some dilutions were performed manually and measured using a microCuvette.



## Automated CG-MALS Measurements

For the automated Calypso measurements, mAb formulations were first diluted in their formulation buffer 2- 5x and filtered to 0.02  $\mu\text{m}$ ; the resulting concentrations are given in Table 1. Automated composition gradients were performed using a Calypso, a DAWN MALS detector with laser power reduced to 50% to prevent signal saturation, and an Optilab refractive index detector with high concentration option. For each composition, the Calypso mixed an aliquot of antibody and buffer and delivered it to the downstream LS and concentration detectors and stopped the flow for 60 seconds. Pump control, data acquisition and analysis were all performed by the CALYPSO software. A typical Calypso method is shown in Figure 2.

	Viscosity (cP)	Max. Conc. for Calypso (mg/mL)
mAb A	~3 (at 100 mg/mL)	43
mAb B	~7 (at 100 mg/mL)	32
mAb C	~13 (at 150 mg/mL)	28

Table 1: Antibody properties and initial dilution for automated measurements

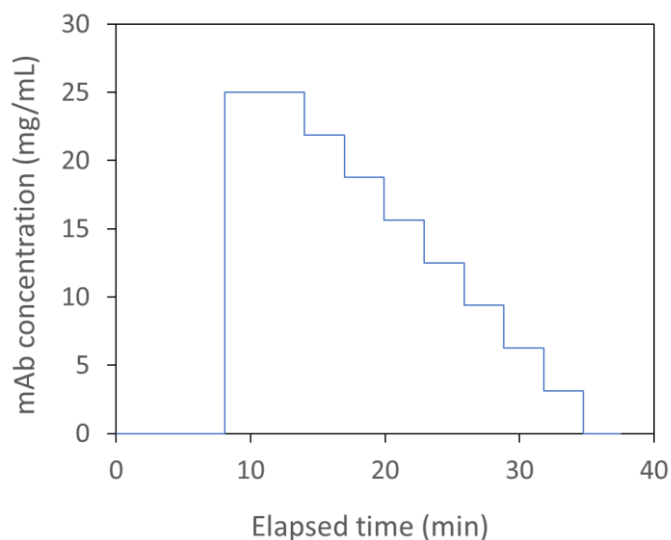


Figure 2: Automated Calypso composition gradient. At each step, the Calypso injected antibody solution at the desired concentration and stopped the flow for 60 seconds to allow for any dissociation kinetics.

## Manual microCuvette Measurements

At the highest concentrations required, the viscosity of mAbs B and C exceeded the capacity of the Calypso. In order to collect additional high concentration data,

dilutions were prepared manually, and light scattering was measured by the DAWN in a microCuvette. mAb A was also measured in this manner for comparability purposes. In preparation for these experiments, mAb A was filtered to 0.1  $\mu\text{m}$  and mAbs B and C were filtered to 0.2  $\mu\text{m}$ . Dilutions of the filtered stock solution were made with buffer filtered to 0.02  $\mu\text{m}$ . To prevent saturation of detector signals at the highest concentrations, the DAWN's laser power was set to 100% for mAb A, 13% for mAb B, and 25% for mAb C.

## Results and Discussion

The difference in intermolecular interactions between the three antibodies is immediately apparent in their light scattering data. Although all three molecules have a monomer molecular weight  $\sim 150$  kDa, the LS signals for mAbs B and C exhibit a significantly different behavior than that of mAb A under the same concentrations (Figure 3). In fact, at  $\sim 100$  mg/mL, the light scattering signal from mAbs B and C is  $\sim 8.5$ -fold that of mAb A. This indicates that mAbs B and C exhibit strong attractive interactions, compared to mAb A. It is plausible to assume that these attractive interactions are the mechanism for their increased viscosity.

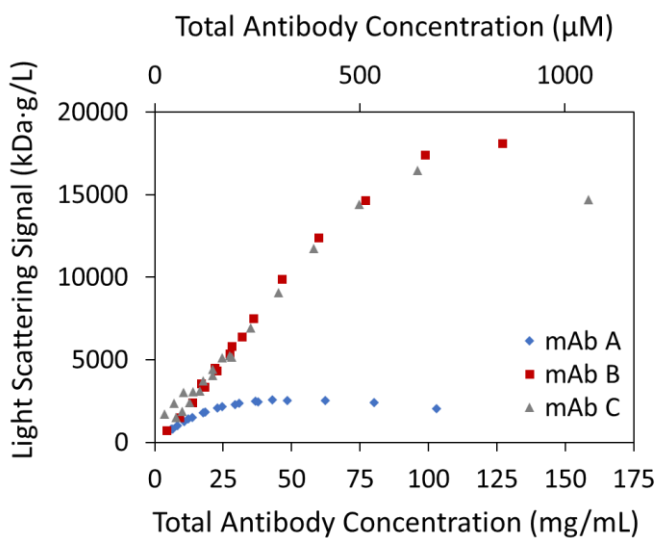


Figure 3: Light scattering signal as a function of concentration for monoclonal antibodies A, B, and C

Data analysis of mAb A, which exhibited the lowest viscosity, indicates no attractive self-interactions. Rather, mAb A experienced only repulsive interactions, quantified by a second virial coefficient  $A_2 = 7.3 \times 10^{-5} \text{ mol} \cdot \text{mL} / \text{g}^2$ . This is equivalent to the excluded volume interactions

exhibited by a hard sphere with molecular weight 150 kDa and radius 5.5 nm. The effective radius is slightly larger than the actual hydrodynamic radius of IgG (which is generally in the range of 4.8 – 5.2 nm as determined by dynamic light scattering), suggesting additional intermolecular repulsion due in all likelihood to partially screened charge-charge repulsion. We note here that while only  $A_2$  is reported, the analysis actually allows for a sixth-order virial expansion where all virial coefficients are calculated from a single free parameter, the hard-sphere specific volume.

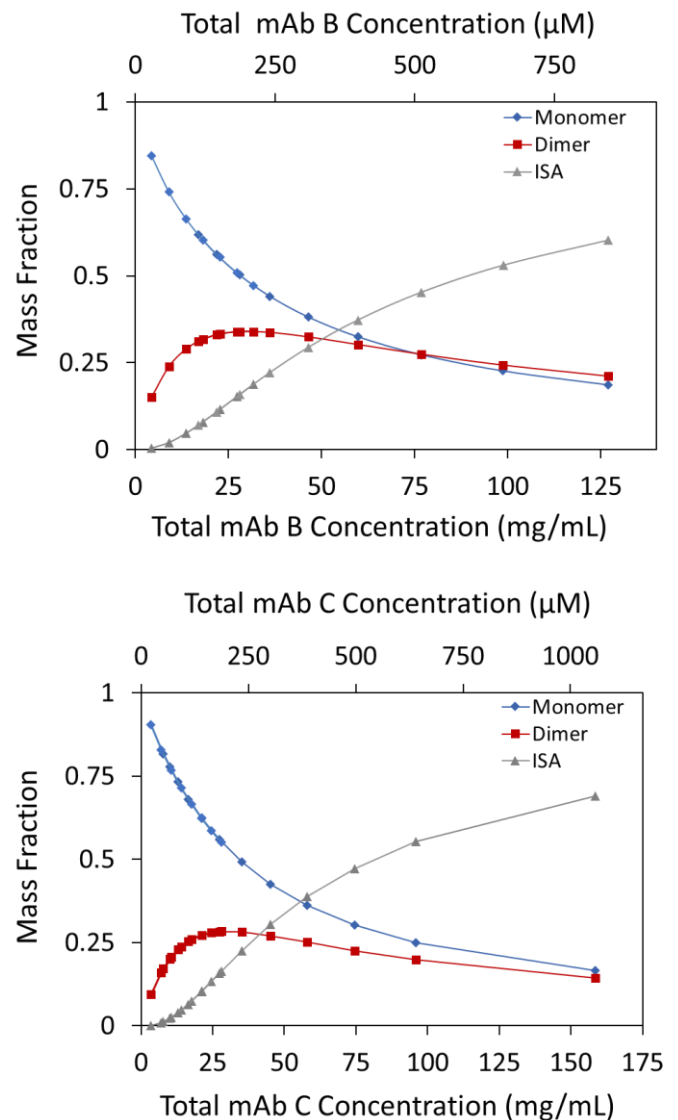


Figure 4: Mass distribution of oligomeric species for mAb B (top) and mAb C (bottom) as derived from fitting the light scattering data vs. concentration to a model that included an equilibrium between monomers, dimers, and infinite self-association (ISA) of dimers. The "ISA" ( $\blacktriangle$ ) curves refer to the mass fraction of all  $n$ -mers, where  $n = 4, 6, 8, \dots$

In contrast, both mAbs B and C appeared to form clusters or loose networks of quasi-specifically associated oligomers (Figure 1). Even in the dilute experiments performed with automated concentration gradients, the apparent molecular weight indicated oligomerization into species with at least dimer molecular weight. After concatenating the data sets obtained in both (lower concentration) automated Calypso-generated gradients and (higher concentration) manual cuvette measurements, several association models were considered for each antibody. As a first pass, the data were fit to models that incorporated dimers, trimers, etc. with arbitrary, independent association constants. Then the model was refined for a particular mechanism of self-association.

In the case of mAb C, the best fit required n-mers with  $n > 6$ . In addition, the curvature in the LS data as a function of concentration was fit best when odd-numbered oligomers were omitted. For this antibody, the best fit to the data was finally accomplished with a model that assumes the following: 1) antibody monomers formed dimers ( $mAb_2$ ) with affinities “Dimerization  $K_d$ ” on the order of several hundred micromolar; 2) these dimers further self-associated to form higher-order oligomers ( $(mAb_2)_n$ ) with an independent affinity “ISA  $K_d$ ”. The dimer-dimer interaction is calculated according to a model of isodesmic, infinite self-association (ISA) wherein each dimer adds to the progressively assembled chain or cluster with equal affinity<sup>5</sup>.

The equilibrium dissociation constants are listed in Table 2. Based on the calculated affinities, mAb C appears to exhibit a small degree of cooperativity: the affinity of dimer-dimer association (“ISA  $K_d$ ”) is higher than that of monomer-monomer (“Dimerization  $K_d$ ”). Though the difference between the two affinities is not great, it is significant within experimental and fitting error. This phenomenon is not unusual and has been considered previously in terms of nucleation models of association [see Reference 5 and references therein].

The same dimer/ISA model also yielded the best fit to the data when applied to mAb B. Figure 4 shows the mass distribution of monomer, dimer, and higher order oligomers (ISA) for each antibody. Based on this model, the molar distribution of each oligomer could be calculated, and for both mAbs B and C, oligomers  $>10$ -mers represented  $<1\%$  mol/mol.

One point of distinction between the two antibodies is the lack of statistically significant difference in mAb B’s Dimerization  $K_d$  and ISA  $K_d$  values. A second point is the viable alternative description of the interactions among mAb B molecules as an isodesmic self-association of monomers (rather than an association of dimers), i.e., monomer mAbs self-assemble progressively with each monomer adding to the growing oligomer with equal affinity ( $K_d = 430 \mu\text{M}$ ). As shown in Figure 5, a model of isodesmic self-association up to 10-mers, though not as good a fit as the dimer self-association scheme, may also be suitable for describing mAb B (dashed red line, Figure 5); however, this model clearly does not agree with the data collected for mAb C. Additional data with mAb B at  $\sim 160 \text{ mg/mL}$  would be required to confirm the association model.

	$A_2$ (mol·mL/g <sup>2</sup> )	Dimerization $K_d$ ( $\mu\text{M}$ )	ISA $K_d$ ( $\mu\text{M}$ )
mAb A	$7.13 \times 10^{-5}$	--	--
mAb B	$4.47 \times 10^{-5}$	280	180
mAb C	$5.09 \times 10^{-5}$	400	130

Table 2: Best fit parameters for self-interactions of mAbs A, B, and C

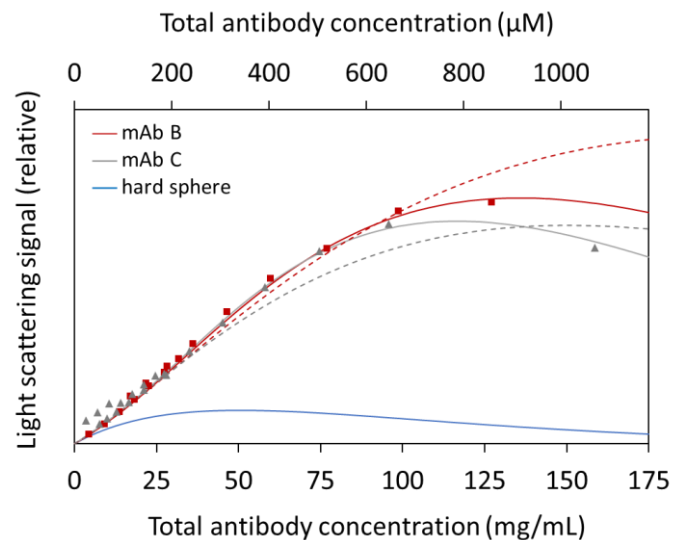


Figure 5: Light scattering data for mAbs B and C best fit to a model of infinite self-association of dimers (solid line) or isodesmic self-association of monomers (dashed line). A model of typical excluded volume repulsion, with no attractive interactions, (e.g., mAb A) is shown for reference.

In addition to the attractive interaction, thermodynamic non-ideality must be taken into account in the form of a

positive second virial coefficient. Here,  $A_2$  quantifies only the portion of the interaction due to nonspecific repulsion, such as excluded volume and charge-charge repulsions. The  $A_2$  values for mAbs B and C were similar (Table 2), and were equivalent to the excluded volume interactions exhibited by a hard sphere with molecular weight 150 kDa and radius 4.7-4.8 nm.

## Conclusions

CG-MALS measurements automated by the Wyatt Calypso provided insight into the mechanism behind the different colloidal behaviors of three antibody solutions. Analysis of CG-MALS data via the CALYPSO software quantified both the attractive and repulsive interactions. The net attractive interactions in formulations B and C correlated to their increased viscosity as compared to mAb A, illuminating the nature of the intermolecular forces that contribute to high viscosity.

To learn more about CG-MALS see [www.wyatt.com/CG-MALS](http://www.wyatt.com/CG-MALS).

For more information on Calypso or to request a quote, please visit [www.wyatt.com/Calypso](http://www.wyatt.com/Calypso).



## References

1. Minton, A. P. Static Light Scattering from Concentrated Protein Solutions, I: General Theory for Protein Mixtures and Application to Self-Associating Proteins. *Biophys. J.* **93**, 1321–1328 (2007).
2. Scherer, T. M., Liu, J., Shire, S. J. & Minton, A. P. Intermolecular Interactions of IgG1 Monoclonal Antibodies at High Concentrations Characterized by Light Scattering. *J. Phys. Chem. B* **114**, 12948–12957 (2010).
3. Some, D. & Kenrick, S. Characterization of Protein-Protein Interactions via Static and Dynamic Light Scattering. *Protein Interact.* (2012) doi:10.5772/37240.
4. Yadav, S., Liu, J., Shire, S. J. & Kalonia, D. S. Specific interactions in high concentration antibody solutions resulting in high viscosity. *J. Pharm. Sci.* **99**, 1152–1168 (2010).
5. Zehender, F., Ziegler, A., Schönfeld, H.-J. & Seelig, J. Thermodynamics of Protein Self-Association and Unfolding. The Case of Apolipoprotein A-I. *Biochemistry* **51**, 1269–1280 (2012).



© Wyatt Technology LLC. All rights reserved. No part of this publication may be reproduced, stored in a retrieval system or transmitted, in any form by any means, electronic, mechanical, photocopying, recording, or otherwise, without the prior written permission of Wyatt Technology.

One or more of Wyatt Technology's trademarks or service marks may appear in this publication. For a list of Wyatt's trademarks and service marks, please see <https://www.wyatt.com/about/trademarks>.